AAPS PharmSciTech, Vol. 10, No. 2, June 2009 (© 2009)
DOI: 10.1208/s12249-009-9249-7

Research Article

Enhancement of Oral Bioavailability of Cilostazol by Forming its Inclusion Complexes

Samir G. Patel[1,3] and Sadhana J. Rajput[2]

Received 11 December 2008; accepted 23 April 2009; published online 21 May 2009

Abstract. The study was designed to investigate the effect of cyclodextrins (CDs) on the solubility, dissolution rate, and bioavailability of cilostazol by forming inclusion complexes. Natural CDs like β-CD, γ-CD, and the hydrophilic β-CD derivatives, DM-β-CD and HP-β-CD, were used to prepare inclusion complexes with cilostazol. Phase solubility study was carried out and the stability constants were calculated assuming a 1:1 stoichiometry. Solid cilostazol complexes were prepared by coprecipitation and kneading methods and compared with physical mixtures of cilostazol and cyclodextrins. Prepared inclusion complexes were characterized by Fourier transform infrared spectroscopy, differential scanning calorimetry (DSC), and X-ray diffraction (XRD) studies. *In vitro* dissolution study was performed using phosphate buffer pH 6.4, distilled water, and HCl buffer pH 1.2 as dissolution medium. The optimized inclusion complex was studied for its bioavailability in rabbit and the results were compared with those of pure cilostazol and Pletoz-50. Phase solubility study showed dramatic improvement in the solubility of drug by formation of complexes, which was further increased by pH adjustment. The dissolution rate of cilostazol was markedly augmented by the complexation with DM-β-CD. DSC and XRD curves showed sharp endothermic peaks indicating the reduction in the microcrystallinity of cilostazol. Selected inclusion complex was also stable at ambient temperature up to 6 months. The *in vivo* study revealed that DM-β-CD increased the bioavailability of cilostazol with low variability in the absorption. Among all cilostazol–cyclodextrins complexes, cilostazol–DM-β-CD inclusion complex (1:3) prepared by coprecipitation method showed 1.53-fold and 4.11-fold increase in absorption along with 2.1-fold and 2.97-fold increase in dissolution rate in comparison with Pletoz-50 and pure cilostazol, respectively.

KEY WORDS: bioavailability; cilostazol–CD inclusion complex; dissolution; solubility; stability study.

INTRODUCTION

Cilostazol,{6-[4-(1-cyclohexyl-1*H*-tetrazol-5-yl)butoxy]-3,4-dihydro-2(1*H*)-quinolinone}(Fig. 1) (1), is a cyclic adenosine monophosphate (cAMP) phosphodiesterase III inhibitor, inhibiting phosphodiesterase activity and suppressing cAMP degradation with a resultant increase in cAMP in platelets and blood vessels, leading to inhibition of platelet aggregation and vasodilation. Cilostazol is slightly soluble in methanol, ethanol, and practically insoluble in water, 0.1 N HCl and 0.1 N NaOH. The reported Log *P* value is 3.048 (http://www.chemspider.com/Search.aspx; accessed August 15 2008). The pharmacokinetic parameters of cilostazol following oral administration are generally highly variable. Peak plasma concentration has been shown to be 1.2 μg/mL after a single oral dose of 100 mg, generally obtained 3 to 4 h after oral administration (1).

Cilostazol absorption in the gastrointestinal tract is slow, variable, and incomplete. A high-fat meal increased absorption, with approximately 90% increase in C_{max} and a 25% increase in area under curve (AUC) (1). The absolute bioavailability of cilostazol is not known and relative bioavailability is unpredictable. After oral administration, approximately 56% cilostazol and its metabolites (19%) are eliminated through urine (74%) and the remaining is excreted in feces (20%). The apparent elimination half-life of cilostazol and its active metabolite is 11–13 h in adults with normal renal functions (1). The aim of the study was to develop the inclusion complexes of cilostazol to enhance the solubility and oral bioavailability.

Cyclodextrins (CDs) are cyclic oligosaccharide consisting of at least six α-(1-4)-linked glucopyranose units. α-, β-, and γ-CD consist of six, seven, and eight glucopyranose units, respectively (2). These are often depicted as hollow truncated cones with exterior hydrophilic surface and an electron-rich hydrophobic interior surface. Exterior hydrophilic surface is favorable for enhancement of absorption rate through the gastrointestinal tract and the hydrophobic cavity generally provides a favorable environment for hydrophobic molecules or parts of a molecule thus improving the solubility of hydrophobic compounds in aqueous solutions (3,4). The solubilization abilities of CDs have been attributed to the formation of inclusion complexes between CDs and the "guest" molecules. Generally, this complexation involves the

[1] Pharmaceutics Department, Ramanbhai Patel College of Pharmacy, Education Campus Changa, Changa. Dist.: Aanand, Gujarat, India.
[2] Pharmaceutical Quality Assurance Laboratory, Pharmacy Department, The M. S. University of Baroda, Vadodara, Gujarat, India.
[3] To whom correspondence should be addressed. (e-mail: samirpatel1602@gmail.com)

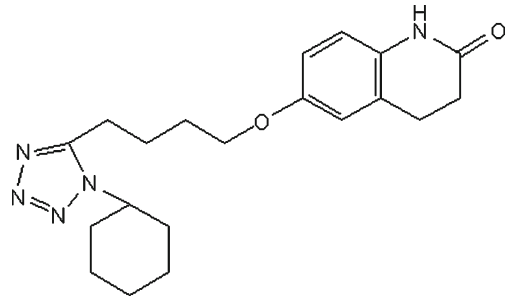

Fig. 1. Chemical structure of cilostazol

inclusion of the "guest" molecule in the cavity of the host molecule, such as CD, with no covalent bonding (5). However, practical use of natural CDs as cilostazol carriers is restricted by their lower aqueous solubility. Several hydrophilic CD derivatives have been used to solve the problem (*i.e.*, the methylated, hydropropylated, and sulfobutyl ether CD derivatives, etc.) (6–8). All these derivatized CDs offer better solubility, higher aqueous stability, and increased bioavailability and have less undesirable side effects compared to natural CDs (9–12).

MATERIAL AND METHODS

Materials

Cilostazol was generously provided by Cadila Pharmaceutical Laboratory, Ahmedabad, India, as a gift sample. β-CD was purchased from Hi-media Laboratories Pvt. Ltd. Mumbai. Hydroxypropyl-β-cyclodextrin (HP-β-CD) was obtained as a gift sample from Sun Pharma Advance Research Company, Vadodara, India. γ-CD and dimethyl-β-cyclodextrin (DM-β-CD) were procured as gift samples from Roquette Pharma, USA. High-performance liquid chromatography (HPLC)-grade methanol and acetonitrile were purchased from SD Fine chemicals (Maharashtra, India). All other chemicals used were of analytical grade and used as received without further purification. Triple-distilled water was used throughout the study. The HCl buffer pH 1.2 and phosphate buffer pH 6.8 were prepared as per IP-1996 procedure (13).

Phase Solubility Study

The analytical method based on UV spectrophotometry was developed before starting the phase solubility study. The calibration curve was prepared by measuring the absorbance of standard methanolic solutions of cilostazol in the concentration range 5–50 μg/mL at 257.00 nm. The method was validated as per the International Conference on Harmonization (ICH) guidelines. The coefficient of determination value (R^2) for the calibration curve was 0.9998. The intraday and interday (3 days, n=3) accuracy was 99.58–100.32% and 99.80–100.4%, respectively. The intraday and interday (3 days, n=3) precision was expressed as relative standard deviation and were in range of 1.39–1.98% and 1.37–1.97%, respectively. The limit of detection (LOD) and limit of quantification (LOQ) of the developed method were 0.231 and 0.770 μg/mL, respectively.

The phase solubility of cilostazol was conducted according to Higuchi and Connors (14). An excess amount of cilostazol (50 mg) was added to 5 mL of water or aqueous solutions of CDs and its derivatives (10–50 mol/L) individually in 10-mL stoppered glass tubes. The tubes were shaken for 24 h at 50 cycles per minute in a water bath at 37±0.5°C. At equilibrium after 2 days, aliquots were withdrawn, filtered (0.45-μm cellulose nitrate filters), and suitably diluted. Concentration of cilostazol was determined spectrophotometrically at 257.0 nm. The phase solubility study was further carried out in HCl buffer pH 1.2 (13) and phosphate buffer pH 6.8 (13).

A plot of total molar concentration of the cilostazol against the total molar concentration of CDs gave phase solubility diagrams from where the apparent solubility constant, K_C, was calculated for all the pH values using their regression lines to the following equation.

$$\text{Stability constant } (K_C) = \frac{\text{Slope}}{S_o(1 - \text{Slope})}$$

Where S_o is the intrinsic solubility of the cilostazol studied under the conditions (15–17).

Preparation of Inclusion Complexes

The CDs used for the preparation of inclusion complexes were β-CD, γ-CD, HP-β-CD, and DM-β-CD. Cilostazol–CDs inclusion complexes were prepared in 1:1, 1:2, and 1:3 molar ratios by using two different methods: (1) kneading method and (2) coprecipitation method and compared with physical mixtures of cilostazol–CDs (18).

(a) Physical mixture

The physical mixtures were prepared by mixing pulverized powder of cilostazol with β-CD, γ-CD, HP-β-CD, and DM-β-CD in different cilostazol to CD ratios like 1:1, 1:2, and 1:3. The mixture was then passed through sieve mesh # 100 and stored in a dessicator until further evaluation.

(b) Kneading method

A paste containing one part of cilostazol and three parts of any one CD like, β-CD, γ-CD, HP-β-CD and DM-β-CD, was introduced in to a kneading machine with progressive addition of the cilostazol. The paste was mixed for 1 h. The viscosity of the mixture was increased indicating the formation of the complex. Auxiliary step involved washing the paste with solvent and water followed by filtration. Finally the paste was dried in an oven at 45°C until dry. The paste was ground to get a fine powder and passed through sieve mesh #100. All the prepared inclusion complexes were stored in dessicator until further evaluation.

(c) Coprecipitation method

In this method, an organic solution of the cilostazol was poured under agitation into an aqueous solution of CD with contentious stirring. A solid inclusion complex was obtained either spontaneously or after evaporation of excess solvent. After the precipitation step, the inclusion complex was thoroughly washed with solvent and water, filtered, and dried to get a pure inclusion complex. Finally, dried complex was

passed through sieve mesh # 100 and stored in dessicator until further evaluation.

Inclusion Efficiency Study

All inclusion complexes of cilostazol and their physical mixtures (25 mg) were separately taken in 25-mL volumetric flasks. Ten milliliters of methanol were added to it, mixed thoroughly, and sonicated for 30 min at ambient temperature. The volume was made up to mark with methanol. An aliquot from the each solution was suitably diluted with methanol to get the final concentration of 10 μg/mL of cilostazol and spectrophotometrically assayed for cilostazol content at 257.00 nm. Inclusion efficiency was calculated using the formula:

$$\text{Inclusion efficiency} = (\text{estimated \% cilostazol content}/\text{theoretical \% cilostazol content}) \times 100$$

Physicochemical Characterization

1. IR spectroscopy study

The infrared (IR) spectra were obtained using a Shimadzu Fourier transform infrared (FTIR)-8400S spectrophotometer with IR solution software (Shimadzu). The samples were prepared by grinding a small amount of the dried sample and the corresponding amount of potassium bromide (2/98 *w*/*w*) in an agate mortar. Data were collected over a spectral region from 4,000 to 650 cm^{-1} with resolution of 4 cm^{-1} and 100 scans.

2. Differential scanning calorimetry

Differential scanning calorimetry (DSC) analysis was performed for pure cilostazol, pure CDs and its derivatives, physical mixtures of cilostazol–CDs, and inclusion complexes using a Shimadzu DSC (Model DT-60) instrument. Samples (0.5–1.0 mg) were weighed on Shimadzu Libror AEG 220 electronic balance and transferred to the aluminum boat, crimped and hermetically sealed by using crimping machine. An empty aluminum boat was used as reference. Samples were heated in sealed aluminum boat at a rate of 10°C/min in a 0–400°C temperature range under nitrogen stream. The analysis was repeated after cooling down to temperature in order to estimate the DSC baseline. The instrument was calibrated using indium (melting point, 156.61°C; enthalpy of fusion, 28.71 J/g) (18,19).

3. X-ray powder diffraction study

X-ray diffraction (XRD) pattern of pure cilostazol, pure CDs and its derivatives, physical mixtures of cilostazol–CDs, and inclusion complexes was collected with a PW1701 diffractometer at 30 mA and 40 kV using CuKα radiation with a graphite monochromator on the diffracted beam. The powdered samples (a fraction of 100–180-μm sieved powder) were deposited on an adhesive support and placed in the diffractometer. XRD patterns were recorded in step scan mode in the range $3° \le 2\theta \le 60°$ with step size 0.06. The scanning rate employed was 1° min^{-1} over the 0–100° diffraction angle (2θ) range. The divergence and receiving slits were chosen in order to ensure a high-resolution mode for the crystalline phases (20).

In Vitro Dissolution Study

Dissolution rate studies were performed in a solution containing HCl buffer pH 1.2, distilled water, or phosphate buffer pH 6.4, 900 mL, at 37±0.2°C, using US Pharmacopeia (USP) XXIII (18,21,22) apparatus (Electrolab, India Programmable tablet dissolution test apparatus USP XXI/XXII, TDT-06P) with a basket rotating (Apparatus I) at 50 rpm. The best results in terms of higher percent drug release, dissolution pattern, and dissolution efficiency were obtained in phosphate buffer pH 6.4. Hence, phosphate buffer pH 6.4 was used as dissolution medium for further studies. Physical mixtures and inclusion complexes, each containing 50 mg of cilostazol, were filled into empty hard gelatin capsule shell and subjected to dissolution study. Samples (5 mL) were withdrawn at 10, 20, 30, 40, 50, 60, 75, 90, 105, and 120 min, filtered through Whatman filter paper no. 41, and assayed spectrophotometrically for cilostazol content at 257.8 nm. The experiments were carried out in triplicate and the maximum mean cumulative percent drug released along with standard deviation (SD) of pure cilostazol, marketed formulation (tablet, Pletoz-50), physical mixtures, and inclusion complexes were identified. The percent dissolution efficiency ($DE_{120\ min.}$) values based on the dissolution data along with SD were calculated as per Khan and Rhodes (23) method and time taken for 50% cilostazol dissolved ($T_{50\%}$ value) was identified from the dissolution profiles. The release kinetics of diffusion was also studied by calculating the regression coefficient for zero-order, first-order, and Higuchi's equations.

Stability Study

Approximately 5 g of the formulation was filled in USP type III glass vial and sealed using VP6 crimp on spray pump fitted with 10-μm actuator. The chemical stability was studied as per ICH guideline (photo stability testing for new drug substances and products Q1A (R2)).The stress stability was conducted at 60±2°C in an incubator and the accelerated stability was studied at 30±2°C/65±5% relative humidity (RH) and 40±2/75±5% RH as per ICH guidelines. The duration of stability was 6 months and samples were withdrawn at predetermined time intervals, after 1, 2, 4, and 6 months. Withdrawn samples were tested for their *in vitro* dissolution study and results were compared with *in vitro* dissolution profiles of the test product before and after stability study as per the SUPAC IR guidelines which assure similarity in the product performance and bioequivalence. The similarity factor f_2 was calculated using the reported equation (24,25) in which initial dissolution data were considered as reference values.

$$f_2 = 50LOG\left\{\left[1 + \frac{1}{n}\sum_{t=1} n(R_t - T_t)^2\right]^{-0.5} \times 100\right\}$$

Where R_t and T_t are the percentage of cilostazol dissolved for reference and test samples at each time point.

An f_2 value between 50 and 100 suggests the dissolution profiles can be considered as similar.

Comparative Bioavailability Study

The pharmacokinetic study was performed using New Zealand rabbits weighing 1.0 to 1.5 kg. All experiments and protocol for this study were approved by the Institutional Animal Ethics Committee, The M. S. University of Baroda, and are in accordance with the committee for the purpose of control and supervision of the experiments on Animal, Ministry of Social Justice and Empowerment, Government of India. The dose for the rabbit was calculated to be 4.66 mg/kg of rabbit weight (26). The study was performed in parallel experiments. The animals were fasted overnight prior to the experiment but had free access to water. The conventional tablet(Platoz-50) powder equivalent to 7.0 mg of cilostazol, cilostazol–DM-β-CD inclusion complex in the ratio of 1:3 (equivalent to 7.0 mg of cilostazol), and pure cilostazol (7.0 mg) were taken and mixed with 1 mL of 0.5% of sodium carboxymethyl cellulose solution. Prepared suspensions were administered orally to the rabbits. There were four groups containing eight rabbits in each group, two rabbits for placebo, two rabbits for pure cilostazol, two rabbits for conventional tablet, and two rabbits for cilostazol–DM-β-CD inclusion complex. The blood samples (approximately 400–500 μL) from rabbits were collected from the marginal ear vein using heparinized needle (20–24 size) at 1, 2, 4, 6, 12, 18, and 24 h after oral administration. The heparinized blood samples were immediately transferred to centrifuge tubes (5 mL) and centrifuged at 20,000 rpm at 0°C for 15 min. Supernatant layer of plasma was separated into another centrifuge tube and stored at −20°C for further experimental procedure.

HPLC analysis for Estimation of Cilostazol in Plasma

Drug concentration from plasma was determined by reverse-phase HPLC using isocratic pump connected to manual rheodyne injector with 20-μL fixed loop and a Phenomenex Luna column (C_{18} ODS 250 mm×4.6 id, 5 μ, Torrance, USA) preceded with ODS guard column (10× 5 mm id). The mobile phase was acetonitrile: water (60:40) with the flow rate of 0.4 mL/min. Chromatograms were recorded by ultraviolet (UV) detection at a fixed wavelength of 254.00 nm. Exactly 0.200 mL of thawed plasma was taken in 5-mL polypropylene centrifuge tube with flat caps by adding 0.4 mL of methyl tertiary butyl ether, and the tube was vortexed for 30 s at high speed. The sample was shaken on a rotating shaker (50 rotations per minute) for 3 min. Finally, the sample was centrifuged for 20 min at 2,000 rpm at 4°C and the clear methyl tert-butyl ether layer was transferred with a calibrated pipette to a disposable glass tube and evaporated under a gentle stream of nitrogen. The dried residue was taken up with 25 μL of mobile phase, and 20 μL of this mixture was injected in the HPLC system. The linearity of this method was in the range of 0.1–20 μg/mL having coefficient of determination value (R^2=0.9989). The average extraction efficiency of cilostazol in plasma was 83.42% to 95.13%. The LOD and LOQ of the developed method were 0.0248 and 0.0845 μg/mL, respectively.

Pharmacokinetic Data Analysis

After oral administration of inclusion complex, marketed formulation, and pure cilostazol, the plasma samples were analyzed by HPLC for their cilostazol content. A curve of cumulative drug absorbed *vs*. time over 0 to 24 h was plotted to calculate the AUC. The pharmacokinetic data were calculated using Microsoft Excel work sheet.

RESULTS AND DISCUSSION

Phase Solubility Studies

The phase solubility profiles for the complex formation between cilostazol and CDs in three aqueous solutions (HCl buffer pH 1.2, distilled water, and phosphate buffer pH 6.8) at 37°C are shown in Fig. 2a–c. Initial studies indicated that cilostazol is chemically stable in water for at least 7 days at 37°C. The extremely low solubility of cilostazol (0.101± 0.004 μg/mL in water at 37°C) was linearly increased in a concentration-dependent manner with the increase in CD concentration. Such linear curves are referred to as A_L-type curves in solubility diagrams (27).The regression coefficient values were (R^2) >0.99 in the specified concentration range (14). These linear cilostazol–CDs curves suggested the formation of 1:1 (mol/mol) cilostazol–CD inclusion complexes at different pH values. The calculated stability constant values are shown in Table I. These results indicated

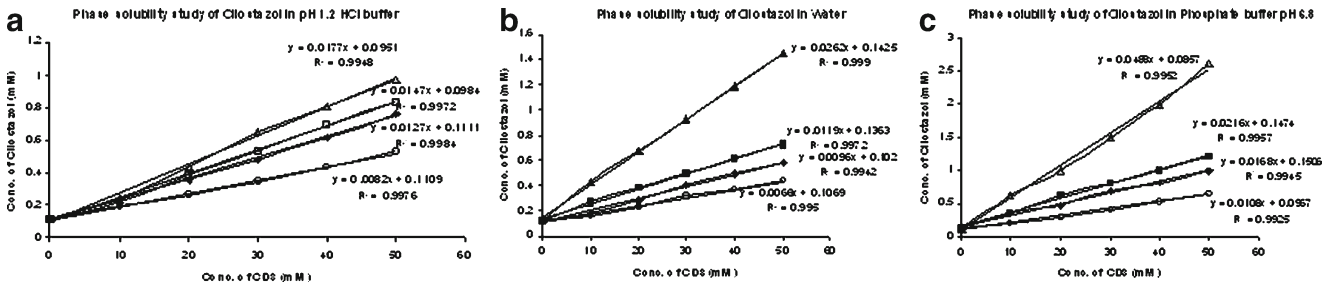

Fig. 2. **a** Phase solubility study of cilostazol in HCl buffer at pH 1.2 at 257.2 nm. Key (*empty triangles*) DM-β-CD; (*empty squares*) HP-CD; (*filled diamonds*) β-CD; (*empty circles*) γ-CD. All values are represented as mean±SD (±*n*=3). **b** Phase solubility study of cilostazol in water at 257.00 nm. Key (*filled triangles*) DM-β-CD; (*filled squares*) HP-CD; (*filled diamonds*) β-CD; (*empty circles*) γ-CD. All values are represented as mean±SD (±*n*=3). **c** Phase solubility study of cilostazol in phosphate buffer at pH 6.8 at 257.8 nm. Key (*empty triangles*) DM-β-CD; (*filled squares*) HP-CD; (*filled diamonds*) β-CD; (*empty circles*) γ-CD. All values are represented as mean±SD (±*n*=3)

Table I. Apparent Inclusion Complex Stability Constant (Kc) of Cilostazol with Different CDs at 37°C and Types of Phase Solubility Curve for Cilostazol with Various CDs at Different pH Solutions

	Cilostazol				
CDs	Solutions	Solubility (μg/mL)	K 1:1 [M^{-1}]±SD[a]	R^2	Type of curve
β-CD	HCl buffer pH 1.2	114.45±6	105.367±7	0.9984	A_L
	Water	87.19±5	79.89±5	0.9942	A_L
	Phosphate buffer pH 6.8	147.74±8	138.804±11	0.9945	A_L
γ-CD	HCl buffer pH 1.2	80.120±3	68.34±6	0.9976	A_L
	Water	66.26±2	55.09±4	0.995	A_L
	Phosphate buffer pH 6.8	98.64±5	89.77±8	0.9925	A_L
HP-β-CD	HCl buffer pH 1.2	125.30±3	121.713±11	0.9972	A_L
	Water	108.58±1	101.81±13	0.9972	A_L
	Phosphate buffer pH 6.8	181.32±8	177.591±15	0.9957	A_L
DM-β-CD	HCl buffer pH 1.2	146.04±6	146.106±17	0.9948	A_L
	Water	217.46±7	214.3997±20	0.999	A_L
	Phosphate buffer pH 6.8	393.52±4	390.071±35	0.9952	A_L

[a] All values are represented as mean±SD (±n=3)

Table II. Inclusion Efficiency Data for Cilostazol CD Inclusion Complexes and Physical Mixtures

Inclusion complexes and physical mixtures of cilostazol CDs (*w*/*w*)			Inclusion efficiency(%)±SD[a]	%RSD[a]
Cilostazol–β-CD (*w*/*w*)	Coprecipitation method	1:1	75.2±2.12	2.16
		1:2	87.4±2.23	2.29
		1:3	98.5±1.50	1.23
	Kneading method	1:1	65.36±2.31	1.88
		1:2	76.96±1.87	1.75
		1:3	85.6±1.53	1.39
	Physical mixture	1:1	55.5±1.50	1.51
		1:2	61.6±0.8	1.05
		1:3	68.5±1.2	1.3
Cilostazol–γ-CD (*w*/*w*)	Coprecipitation method	1:1	69.2±0.92	1.36
		1:2	80.4±0.83	1.89
		1:3	99.4±2.06	2.23
	Kneading method	1:1	71.41±1.34	1.58
		1:2	79.73±1.66	1.63
		1:3	89.1±1.87	2.12
	Physical mixture	1:1	49.2±1.53	1.81
		1:2	58.9±0.85	1.55
		1:3	67.5±1.72	0.83
Cilostazol–HP-β-CD (*w*/*w*)	Coprecipitation method	1:1	67.6±2.32	1.31
		1:2	83.94±1.66	2.39
		1:3	98.9±0.81	1.69
	Kneading method	1:1	61.49±1.82	1.43
		1:2	74.38±2.03	2.12
		1:3	88.0±1.92	1.88
	Physical mixture	1:1	57.50±1.23	1.91
		1:2	79.1±1.35	1.55
		1:3	84.7±1.92	1.23
Cilostazol–DM-β-CD (*w*/*w*)	Coprecipitation method	1:1	77.2±1.12	1.96
		1:2	89.4±1.33	1.89
		1:3	99.64±1.86	1.73
	Kneading method	1:1	80.46±2.19	1.87
		1:2	84.37±1.93	1.56
		1:3	89.13±1.36	1.67
	Physical mixture	1:1	68.7±0.50	2.51
		1:2	79.3±0.45	1.65
		1:3	88.9±0.2	2.39

[a] The results are mean values±SD derived from three different experimental batches

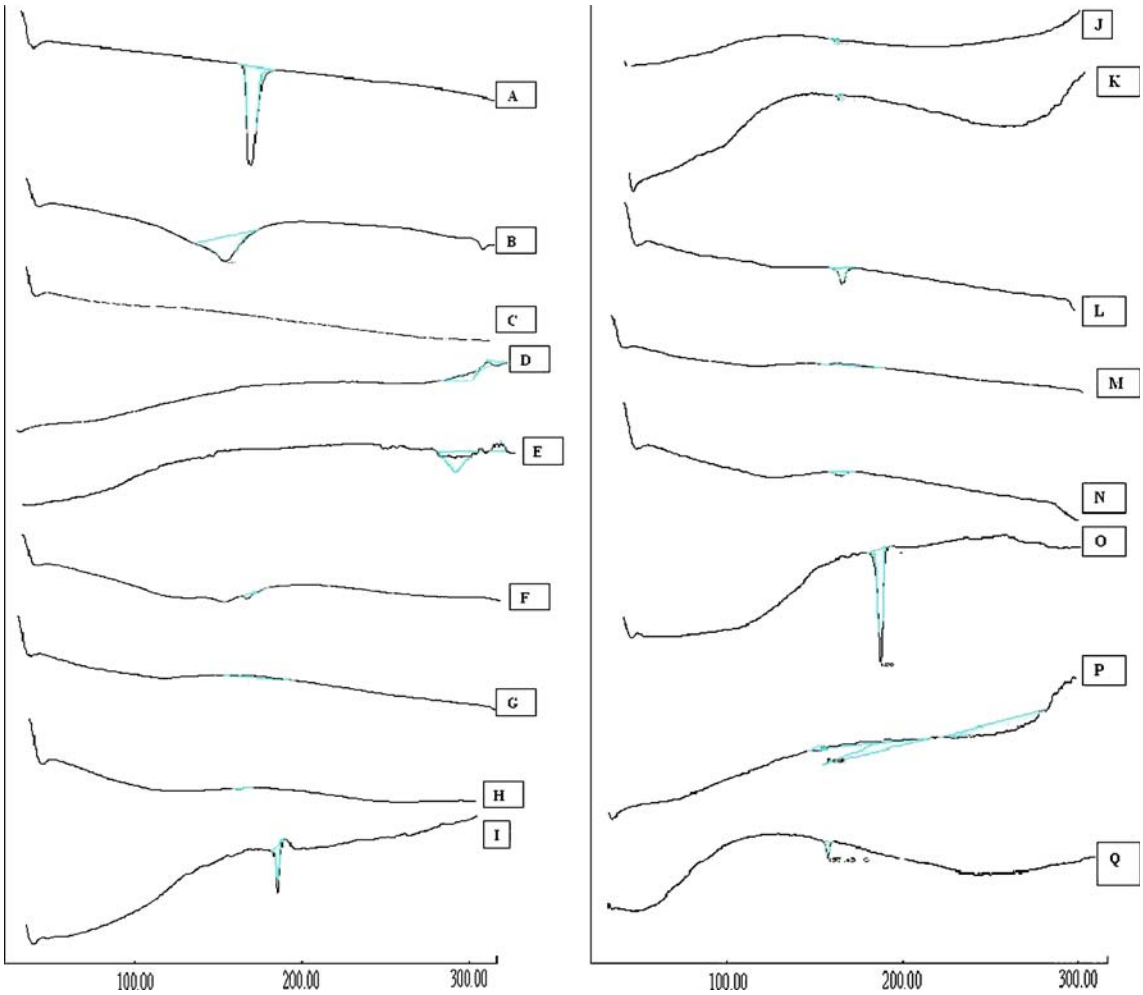

Fig. 3. DSC thermograms of [*A*] pure cilostazol, [*B*] pure β-CD, [*C*] pure γ-CD, [D] pure HP-β-CD, [*E*] pure DM-β-CD, [*F*] cilostazol–β-CD physical mixture (1:3), [G] cilostazol–β-CD inclusion complex by coprecipitation method (1:3), [*H*] cilostazol–β-CD inclusion complex by kneading method (1:3), [*I*] cilostazol–γ-CD physical mixture (1:3), [*J*] cilostazol–γ-CD inclusion complex by coprecipitation (1:3), [*K*] cilostazol–γ-CD inclusion complex by kneading method (1:3), [*L*] cilostazol–HP-β-CD physical mixture (1:3), [*M*] cilostazol–HP-β-CD inclusion complex by coprecipitation method (1:3), [N] cilostazol–HP-β-CD inclusion complex by kneading method (1:3), [O] cilostazol–DM-β-CD physical mixture (1:3), [P] cilostazol–DM-β-CD inclusion complex by coprecipitation method (1:3), [Q] cilostazol–DM-β-CD inclusion complex by kneading method (1:3)

that cilostazol–CD complexes (1:1 molar ratio) were sufficiently stable in phosphate buffer pH 6.8. The solubility of cilostazol was highest (393.52±4 μg/mL) in phosphate buffer pH 6.8 with stability constant value of 390.071±35 M^{-1}.

Inclusion Efficiency Study

The results of inclusion efficiency study are shown in Table II. The data indicate that the percent inclusion efficiency of 1:3 cilostazol–CD inclusion complexes prepared by coprecipitation method was more than 98.5%±1.50, whereas other inclusion complexes prepared by kneading method and physical mixtures have values in the range of 49.2%±1.53 to 89.4%±1.33 suggesting that cilostazol was uniformly distributed in all 1:3 inclusion complex whereas the inclusion complexes and physical mixtures prepared in other ratios did not show satisfactory drug incorporation.

Physicochemical Characterization

FTIR Spectroscopy

Pure cilostazol was characterized by aromatic and aliphatic C–H stretching peaks at 2,867 to 3,315 cm^{-1}, C=N stretching of tetrazole at 1,757 cm^{-1}, N–H stretching of quinolinone at 3,315 cm^{-1}, N=N stretching of tetrazole at 1,687 cm^{-1}, aliphatic C=O stretching band at 1,822.61 cm^{-1}, and aromatic C=C stretching band at 1,506 cm^{-1}. The FTIR spectra of β-CD, γ-CD, HP-β-CD, and DM-β-CD showed intense bands at 3,465–3,247 cm^{-1} corresponding to absorption by hydrogen-bonded OH groups. The bonds that appeared at 3,000–2,800 cm^{-1} were assigned to stretching vibration of the bonds in –CH and $–CH_2$ groups. In the physical mixtures of cilostazol–CDs, the spectra were the superimpositions of those of the pure compounds with

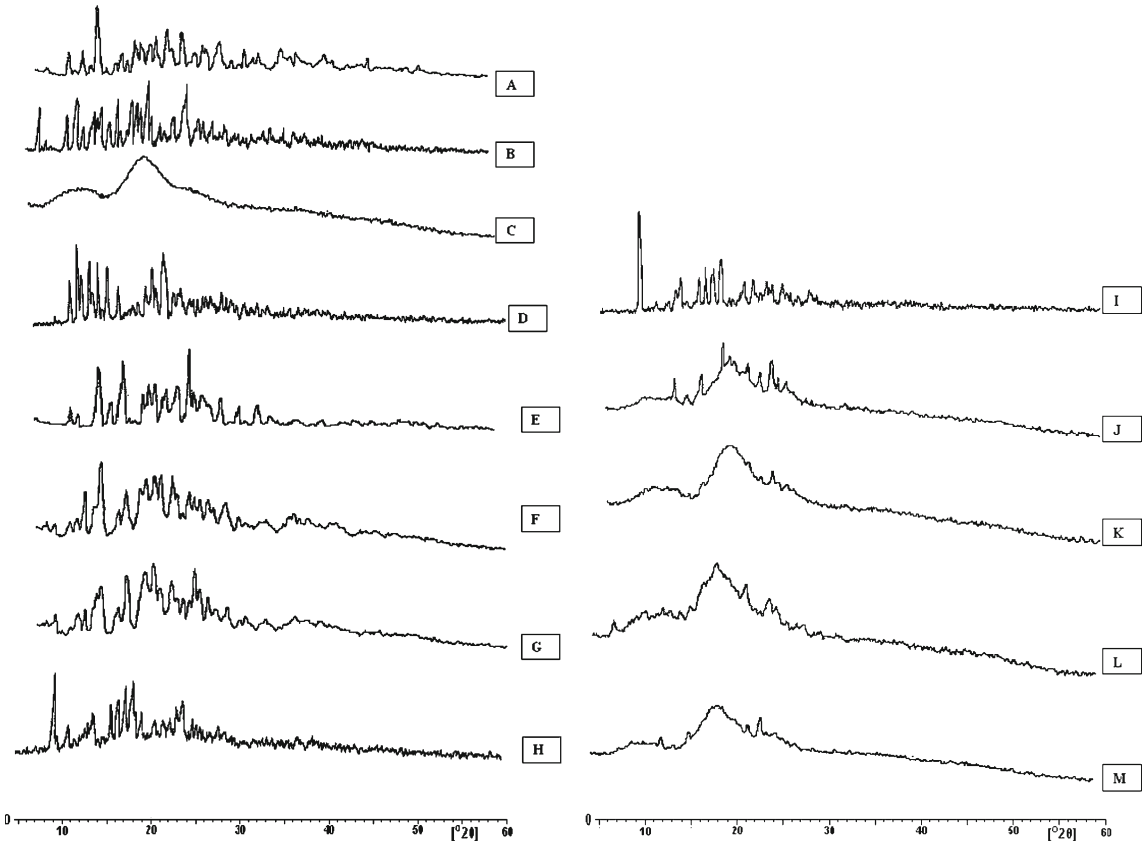

Fig. 4. X-ray diffraction patterns of [*A*] pure β-CD, [*B*] pure γ-CD, [*C*] pure HP-β-CD, [*D*] pure DM-β-CD, [*E*] pure cilostazol, [*F*] cilostazol–β-CD physical mixture (1:3), [*G*] cilostazol–β-CD inclusion complex (1:3), [*H*] cilostazol–γ-CD physical mixture (1:3), [*I*] cilostazol–γ-CD inclusion complex (1:3), [*J*] cilostazol–HP-β-CD physical mixture (1:3), [*K*] cilostazol–HP-β-CD inclusion complex (1:3), [*L*] cilostazol–DM-β-CD physical mixture (1:3), [*M*] cilostazol–DM-β-CD inclusion complex (1:3)

attenuation of the cilostazol peaks. However, the spectra of inclusion compounds showed rightward shifts of the band corresponding to hydrogen-bonded OH groups (from 3,352.05 to 3,315 cm^{-1} for the cilostazol–β-CD complex, from 3,380 to 3,340 cm^{-1} for the cilostazol–γ-CD complex, from 3,380.98 to 3,313 cm^{-1} for the cilostazol–HP-β-CD complex, and from 3,465.84 to 3,461.99 cm^{-1} for the cilostazol–DM-β-CD complex). These results suggested that some of the existing bond formed between the OH groups on the narrow side of CD molecules might be disturbed after the formation of inclusion complexes.

Differential Scanning Calorimetry

Evidence for the interaction between cilostazol and CDs can be identified by DSC study and obtained thermograms

Table III. Maximum Percent Cumulative Drug Release of all Physical Mixtures, Inclusion Complexes, Pletoz-50, and Pure Cilostazol

Method	Cilostazol– CDs ratios	Maximum percent cumulative drug release±SD[a]			
		Cilostazol–β-CD	Cilostazol–γ-CD	Cilostazol–HP-β-CD	Cilostazol–DM-β-CD
Physical mixture	1:1	45.35±1.59	51.98±2.62	61.55±1.45	53.22±0.13
	1:2	56.67±1.93	56.09±1.55	66.56±1.59	69.76±0.25
	1:3	69.32±1.75	71.13±1.24	72.34±2.14	78.62±1.78
Kneading method	1:1	47.83±1.47	63.99±1.04	55.76±1.85	61.96±2.85
	1:2	63.76±1.65	66.4±2.33	70.5±2.67	73.61±1.33
	1:3	73.28±1.93	83.72±1.24	79.89±1.24	84.86±1.23
Coprecipitation method	1:1	69.32±1.75	67.87±1.82	78.32±0.830	78.21±2.56
	1:2	68.88±1.56	78.95±1.64	83.72±1.24	88.55±2.14
	1:3	76.49±1.09	87.08±2.02	95.20±2.31	98.16±2.24

PLETOZ 50=46.56±2.1; pure cilostazol=32.98±0.91

[a] The results are mean values±SD derived from three different experimental batches

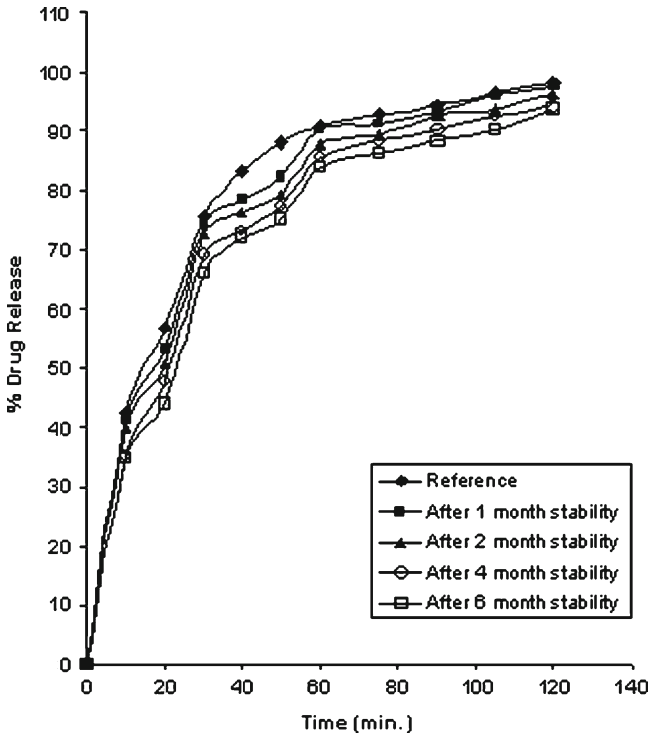

Fig. 5. Cumulative percent drug released from cilostazol–DM-β-CD inclusion complex (1:3) by coprecipitation method for stability study at different time intervals. The results are mean values±SD derived from three different experimental batches

are shown in Fig. 3. Thermogram of pure cilostazol shows a characteristic endothermic peak at 165.13°C corresponding to its melting point. The DSC thermogram of β-CD has large broad endothermic peak between 130.00°C and 160.00°C (148.59°C) that was related to the loss of hydration water of the starting material (20,28,29). β-CD decomposes at about 300.00°C, so there was no trace of melting peak of β-CD in the chosen temperature range, while any endothermic peak was not observed in γ-CD, HP-β-CD, and DM-β-CD. The cilostazol endothermic peak and the β-CD dehydration peaks though rudimentary were observed in the thermogram of the physical mixture of cilostazol with β-CD suggesting the partial complexation. This may be due to the right proportion of β-CD and cilostazol and the appropriate cavity size of β-CD. Cilostazol endothermic peak between 162°C and 165°C was observed in all physical mixtures of γ-CD, HP-β-CD, and DM-β-CD suggesting partial interaction between cilostazol and CDs in these systems. DSC spectra of inclusion complex prepared by coprecipitation method showed complete disappearance of cilostazol endothermic peak in all 1:3 ratios of cilostazol–CDs, while partial inclusion complex formation was observed from the DSC thermograms of all cilostazol–CDs inclusion complexes prepared by kneading method. From all the data, it can be concluded that coprecipitation method was the most suitable method for the formation of cilostazol–CD inclusion complexes.

X-ray powder diffraction study

Powder XRD study was used to measure the crystallinity of the formed inclusion complexes. The peak position (angle of diffraction) is an identification tool of a crystal structure, whereas the number of peaks is a measure of sample crystallinity in a diffractogram. The formation of an amorphous state proves that the drug was dispersed in a molecular state with CD. All the XRD patterns of cilostazol–CDs inclusion complexes and physical mixtures are shown in Fig. 4. The powder X-ray diffraction pattern of pure cilostazol exhibited a series of intense peaks at 2θ value of 12.67, 12.98, 15.35, 15.76, 17.98, 18.71, 19.52, 22.19, and 22.58 which were indicative of their crystallinity. However, the patterns of β-CD, γ-CD, and DM-β-CD are all crystalline in nature while only HP-β-CD was amorphous. In physical mixtures of cilostazol–CDs, most of the principal peaks of cilostazol and CDs are present and the curves are approximate superimposition of the pattern of the raw materials. This indicated partial interaction between the pure components in physical mixtures.

On the other hand, inclusion complexes of cilostazol–HP-β-CD and cilostazol–DM-β-CD in the ratio of 1:3, prepared by coprecipitation method, have completely diffused diffraction patterns. These results suggested the formation of amorphous inclusion complexes, whereas the diffraction patterns of inclusion complexes of cilostazol–β-CD and cilostazol–γ-CD in the ratio of 1:3 were completely different from that of pure cilostazol, β-CD, γ-CD, and its physical mixtures, suggesting the formation of partial inclusion complexes. Hence, it was concluded that HP-β-CD and DM-β-CD are the suitable excipients for the preparation of cilostazol inclusion complexes.

In Vitro Dissolution Study

In vitro dissolution study of the drug in aqueous solution is the rate-limiting step for the absorption of poorly water soluble drugs. In the phase solubility study, it was suggested that the phosphate buffer pH 6.4 was the most suitable dissolution medium as it showed maximum drug release. Dissolution study in phosphate buffer pH 6.4 was carried out for all cilostazol–CD physical mixtures and inclusion complexes prepared in different ratios (1:1, 1:2, and 1:3) by using coprecipitation and kneading methods. The dissolution profiles of cilostazol–CDs (inclusion complex and physical mixtures) are compared with that of marketed formulation and pure drug. The maximum mean cumulative percent drug released±SD for 120 min for all the ratios are shown in Table

Table IV. Similarity Factor (f_2) and Student's T Test Values for the Stability Profile of Cilostazol–DM-β-CD Inclusion Complex (1:3) by Coprecipitation Method for 6 Months

Batch	f_2	T stat	T cri
Reference batch compared with after 6 months of storage batch	66.85	0.5990	2.0859

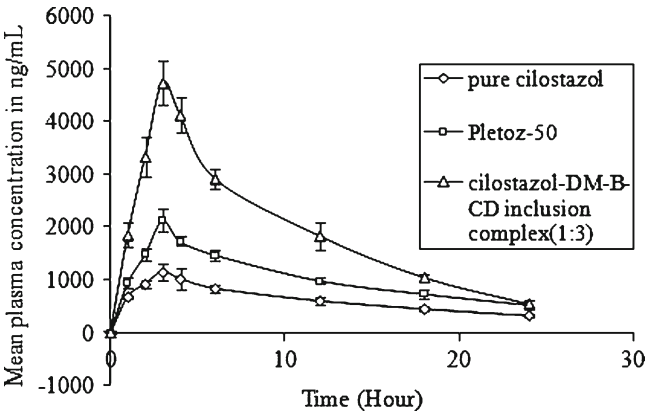

Fig. 6. Comparison of pharmacokinetic profiles of pure cilostazol, conventional tablet, and cilostazol–DM-β-CD inclusion complex

III. It is evident from the data that optimized cilostazol–CD inclusion complexes prepared by coprecipitation method showed better drug release than other inclusion complexes, physical mixtures, marketed formulation (Pletoz-50), and drug solution. Cilostazol–DM-β-CD inclusion complex (1:3ratios) showed a 2.10-fold substantially higher drug release compared to Pletoz-50 and 2.97-fold higher drug release compared to cilostazol solution. The graphs of percent drug dissolved *vs*. time were found to be nonlinear, suggesting that the dissolution pattern did not follow zero-order kinetics. However, the correlation coefficients indicated that Higuchi's model was found to be the best-fit curve compared with zero-order and first-order kinetic for all the tested formulations. The values of $DE_{120\ min}$ and T_{50} study for cilostazol–CDs physical mixtures, inclusion complexes, cilostazol, and Pletoz-50 showed that inclusion complex of cilostazol–DM-β-CD in the ratio of 1:3, prepared by coprecipitation method, was having the highest dissolution efficiency (89.59%) and lowest time taken for 50% dissolution (T_{50} value 11.81 min) and indicated that the inclusion complex of cilostazol–DM-β-CD (1:3) prepared by coprecipitation method was having a rapid and higher dissolution rate among all inclusion complexes and physical mixtures.

Stability Study

Cilostazol–DM-β-CD inclusion complex having a ratio of 1:3 prepared by coprecipitation method showed satisfactory *in vitro* dissolution results; hence, it was evaluated for chemical stability study. The study was carried out as per ICH Q1A (R2) and SUPAC IR guidelines and the withdrawn samples up to 6 months were characterized by *in vitro* dissolution study. Obtained data are represented in Fig. 5, which shows that the change of cumulative percentage of drug release after 6 months was from 2.0% to 5.0%. The dissolution curve also showed similar changes in dissolution patterns indicating that cilostazol was stable in the inclusion complex. The results of Student's *t* test and similarity factor (f_2) are mentioned in Table IV showing insignificant difference between the dissolution profiles. The calculated f_2 values for the batches are higher than 50. It can be concluded from the data that there is insignificant change in the formulated product on storage.

Comparative Bioavailability Study

Cilostazol–DM-β-CD inclusion complex (1:3) prepared by coprecipitation method showed satisfactory results in all preliminary studies; hence, it was selected for *in vivo* absorption studies. The plasma concentration *vs*. time profile after 24 h is shown in Fig. 6 and the pharmacokinetic parameters are mentioned in Table V. The results show that the C_{max} of cilostazol–DM-β-CD inclusion complex is 2.23-fold higher than marketed formulation (Pletoz-50) and 4.11-fold higher than pure cilostazol. The value of $T_{1/2}$ was also decreased in cilostazol–DM-β-CD inclusion complex (7.46 h) compared with Pletoz-50 (11.83 h) and pure cilostazol (12.68 h). Relative bioavailability of cilostazol inclusion complex was 1.53 times higher than marketed formulation. A sharp reduction in $T_{1/2}$ value indicated faster *in vivo* absorption compared to Pletoz-50 and pure cilostazol. The enhancement of oral absorption rate may be attributed to (1) complete cilostazol incorporation into CD, (2) improved dissolution because of the hydrophilic exterior surface of

Table V. Different Pharmacokinetic Parameters of Cilostazol in Rabbits after Oral Administration of 4.66 mg/kg of Cilostazol

Parameters #	Pure cilostazol	Marketed formulation (Platoz-50)	Cilostazol–DM-β-CD inclusion complex (1:3)
C_{max} (ng/ml)	1,150.96±101*	2,126.48±185*	4,734.88±252*
t_{max} (h)	3.90±1.32	4.00±0.93	3.50±0.66
k_a (h^{-1})	0.77±0.006	0.63±0.003	0.71±0.001
k_{el} (h^{-1})	0.05±0.002	0.06±0.0032	0.09±0.0022
$T_{1/2}$ (h)	12.68±1.84*	11.83±1.56*	7.46±1.58*
V_d (L)	1.2573±0.03	0.7305±0.05	0.3020±0.007
$AUC_{0\to\infty}$ (ng h ml^{-1})	21,007.19±1543	34,197.55±1383	52,625.59±1482
MRT (h)	9.62±1.32	9.51±1.56	8.57±2.01
Cl (ml h^{-1})	0.07±0.002	0.04±0.001	0.03±0.0023
TCR (L/h)	0.07±0.004	0.04±0.004	0.03±0.0015
Relative bioavailability[a]	–	–	1.53

Mean±SD, $n=6$
AUC area under the curve, *MTR* mean residence time, *Cl* clearance, *TCR* total clearance rate
[a] Relative bioavailability=$(AUC_{Inc.\ Comp}/AUC_{TAB})\times(dose_{TAB}/dose_{Inc.Comp})$
*$p<0.05$ (ANOVA test)

CD, and (3) the stability of inclusion complex in the gastrointestinal tract.

CONCLUSION

Cilostazol formed its inclusion complexes in either its neutral or charged form with DM-β-CD and HP-β-CD. γ-CD having larger cavity size was not suitable for the formation of inclusion complex with cilostazol. The interaction between cilostazol and DM-β-CD was stronger than HP-β-CD and neutral CDs. Data obtained from the IR, DSC, and X-ray studies showed that it is possible to form inclusion complex between cilostazol and CDs and the coprecipitation technique produced amorphous complexes. DM-β-CD improved the oral bioavailability with low variability *in vivo* as evidenced by the faster dissolution rate of cilostazol. A shorter $T_{50\%}$ of dissolution is found for the formulation prepared by coprecipitation method. All the obtained data suggested that the cilostazol–DM-β-CD inclusion complex (1:3) prepared by coprecipitation method may have grater utility in the fast-dissolving dosage forms with possible enhancement of oral bioavailability.

ACKNOWLEDGEMENT

The authors are thankful to The Maharaja Sayajirao University of Baroda for providing financial support to one of the author (S.G.P.). The authors are also thankful to Roquette Pharma, U.S.A., and Sun Pharma Advance Research Center, Vadodara, India for their generous gift of γ-CD, DM-β-CD, and HP-β-CD and to Cadila Pharmaceuticals, Ahmedabad, India for providing the gift sample of cilostazol. Our sincere thanks to Food and Drug Laboratory, Vadodara, for providing necessary facilities for animal study in the laboratory.

REFERENCES

1. Medical EconomicsPhysicians. Physicians' desk reference. 59th ed. Stamford: Thomson; 2005. p. 2564–6.
2. Larsen KL. Large cyclodextrins. J Inclusion Phenom Macro Chem. 2002;43(1–2):1–13.
3. Szejtli J, Osa T. Comprehensive supramolecular chemistry: cyclodextrins, vol 3. Oxford: Pergamon; 1996.
4. Uekama K, Hirayama F, Irie T. Cyclodextrin drug carrier systems. Chem Rev. 1998;98(5):2045–76.
5. Mosher G, Thompson D. Complexation and cyclodextrins. encyclopedia of pharmaceutical technology, Vol. 19. New York: Marcel and Dekker; 1999. p. 49–88.
6. Homans SW. A molecular mechanical force field for the conformational analysis of oligosaccharides: comparison of the theoretical and crystal structure of Manα1–3Manβ1–4GlcNAc. Biochemistry 1990;29(39):9110–8.
7. Zuo Z, Kwon G, Stevenson B, Diakur J, Wiebe LI. Flutamide-hydroxypropyl-β-cyclodextrin complex: formulation, physical characterization, and absorption studies using the Caco-2 *in vitro* model. J Pharm Pharmceut Sci. 2000;3(2):220–7.
8. Dollo G, Corre PL, Chollet M, Chevanne F, Bertault M, Burgot JL, *et al.* Improvement in solubility and dissolution rate of 1,2-dithiole-3-thiones upon complexation with β-cyclodextrin and its hydroxypropyl and sulfobutyl ether-7 derivatives. J Pharm Sci. 1999;88:889–95.
9. Duchene D. New trends in cyclodextrins and derivatives. Paris: Editios de Sante; 1992. p. 351–407.
10. Fromming KH, Szejtli J. Cyclodextrins in pharmacy (Topics in inclusion science). Dordrecht: Kulwer Academic; 1994.
11. Thompson DO. Cyclodextrin-enabling excipients: their present and future use in pharmaceuticals. Crit Rev Ther Drug Carrier Syst. 1997;14:1–104.
12. Masson M, Loftsson T, Masson G, Stefansson E. Cyclodextrin as permeation enhancer: some theoretical evaluations and *in vitro* testing. J Control Release 1999;59(1):107–18.
13. Govt. of India, Ministry of Health and Family Welfare. Pharmacopoeia of India, vol I. 4th ed. New Delhi: Controller of Publication; 1996. p. A–144–7.
14. Higuchi T, Connors KA. Phase solubility techniques. Adv Anal Chem Inst. 1965;4:117–212.
15. Attama AA, Ndibe ON, Nnamani PO. Studies on diclofenac β-cyclodextrin inclusion complexes. J Pharm Res. 2004;3:47–9.
16. Liu X, Lin HS, Thenmozhiyal JC, Chan SY, Ho PC. Inclusion of acitretin cyclodextrins: phase solubility, photostability, and physicochemical characterization. J Pharm Sci. 2003;92(12):2449–57.
17. Hidetoshi A, Kiyokazu Y, Kouzou M, Tetsumi I, Fumitoshi H, Kaneto U. Comparative studies of the enhancing effect of cyclodextrins on the solubility and oral bioavailability of tacrolimus rats. J Pharm Sci. 2001;90(6):690–701.
18. Rawat S, Jain SK. Roficoxib-beta cyclodextrin inclusion complex for solubility enhancement. Pharmazie. 2003;58(9):639–41.
19. Manca ML, Zaru M, Ennas G, Valenti D, Sinico C, Loy G, Fadda AM. Diclofenac-β-cyclodextrin binary systems: physical characterization and *in vitro* dissolution and diffusion studies. AAPS Pharm Sci Tech. 2005;6(3):E464–72.
20. Castro-Hermida JA, Gomez-Couso H, Ares-Mazas ME, Gonzalez-Bedia MM, Castaneda-Cancio N, Otero-Espinar FJ, *et al.* Anticryptosporidal activity of furan derivative G1 and its inclusion complex with beta-cyclodextrin. J Pharm Sci. 2004;93 (1):197–206.
21. Nalluri BN, Chowdary KPR, Murthy KVR, Satyanarayana V, Hayman AR, Becket G. Inclusion complexation and dissolution properties of nimesulide and meloxicam-hydroxypropyl-β-cyclodextrin binary systems. J Inclusion Sci Macro Chem. 2005;53(1–2):103–10.
22. United State Pharmacopoeia. Dissolution study, XXIII, NF XVIII. Rockville: USP Convention; 1995. p. 1791–9.
23. Khan KA, Rhodes CT. Concept of dissolution efficiency. J Pharm Pharmacol. 1975;27(1):48–9.
24. Moore JW, Flanner HH. Mathematical comparison of dissolution profiles. Pharm Technol. 1996;20(6):64–74.
25. Shah VP, Tsong Y, Sathe P, Liu JP. *In vitro* dissolution profile comparison—statistics and analysis of the similarity factor (f_2). Pharm Res. 1998;15(6):889–96.
26. Gibaldi M, Perrier D. Pharmacokinetics (Drugs and the pharmaceutical sciences), 2nd edn, vol. 15. New York: Marcel Dekker, 1982, revised and expanded.
27. Challa R, Ahuja A, Ali J, Khar RK. Cyclodextrins in drug delivery: an updated review. AAPS Pharm Sci Tech. 2005;06(02):E329–57.
28. Wan-Liang L, Qiang Z, Li Z, Hua W, Rong-Yu L, Li-Feng Z, et al. Antipyretic, analgesic and anti-inflammatory activities of ketoprofen β-cyclodextrin inclusion complexes in animals. Bio Pharm Bull. 2004;27(10):1515–20.
29. Ali H, Marzouqi A, Shehatta I, Jobe B, Dowaidar A. Phase solubility and inclusion complex of itraconazole with β-cyclodextrin using supercritical carbon dioxide. J Pharm Sci. 2006;95 (2):292–304.